ARTICLE OPEN

Check for updates

LdIL-2 treatment in ASD: a novel immunotherapeutic approach targeting Th/Treg dysfunction and neuroinflammation

Meng Li[1,3], Xiuying Kui[1,3], Shujun Yang[1], Zuqing Nie[1], Huiling Chen[1], Penghao Yao[1], Xinyi Xu[1], Chen Shen[1], Zhiwei Li[1], Huijia Zhao[1], Jie Wen[1], Xinwei Huang[1], Jingrui Yang[1], Jinyuan Yan[1], Pengfei Wang[1], Bin Li[2]✉ and Xia Cao[1]✉

A significant proportion of children with Autism Spectrum Disorder (ASD) present with immune imbalances. In this study, we sought to alleviate the core symptoms of autism by addressing immune dysregulation, especially T-cell subpopulation imbalances, in BTBR mice through low-dose IL-2 (LdIL-2) treatment. LdIL-2 (30,000 IU) was administered subcutaneously, and changes in autistic behaviors were observed before and after treatment. Behavioral assessments included the three-chamber test, self-grooming test, sniffing test, marble burying test, open field test and Y-maze test. We also examined alterations in peripheral Th/Treg ratios, cytokine levels, and M1/M2 microglia ratios in the central nervous system via flow cytometry. Neuroinflammatory proteins in cerebrospinal fluid were assessed using proteomic analysis. Furthermore, $CD25^+$ Treg cells were depleted using PC61, followed by LdIL-2 intervention, to determine the role of Treg cells in LdIL-2-treated BTBR mice. Our results demonstrated that LdIL-2 significantly ameliorated core symptoms of autism in BTBR mice. LdIL-2 treatment increased Treg cell levels, restored Th17/Treg and Tfh/Treg balance, and corrected immune dysregulation. Central nervous system inflammation was reduced in mice. However, the behavioral improvements were diminished when Treg cells were depleted by PC61. This study represents the first attempt to treat ASD using LdIL-2. The treatment proved safe and effective in improving both core symptoms and immune imbalances in autism. Symptom improvement was linked to increased Treg cell levels in peripheral blood. LdIL-2 shows potential as a novel therapy for addressing core symptoms of autism.

Translational Psychiatry (2025)15:376 ; https://doi.org/10.1038/s41398-025-03609-8

INTRODUCTION

Autism Spectrum Disorder (ASD), characterized by cognitive and behavioral anomalies, is one of the numerous neurodevelopmental disorders affecting humans. Children with ASD often experience deficits in cognitive and communicative abilities, alongside impaired social skills and repetitive, stereotypical behaviors. Pharmacological interventions, such as aripiprazole and risperidone, have been approved to reduce ASD-related behaviors, although these treatments are associated with side effects [1]. Cell therapy has demonstrated that stem cells may attenuate the pro-inflammatory state by modulating the expression of inflammatory markers in children with ASD [2]. Additionally, neurotransmitter regulation, primarily targeting the GABAergic system, has shown potential in improving certain social and memory deficits, associated with ASD [3]. Other biological therapies aim to treat ASD by targeting various pathways and mechanisms, including MAPK, mTOR, and PPAR signaling. However, many of these treatments have limited efficacy in addressing the core symptoms of ASD, and often come with undesirable side effects. As a result, there remains an urgent need for safe and effective treatments that address the core behaviors of ASD. Research has revealed that ASD may be accompanied by immune system dysregulation, including altered cytokines and chemokine profiles, impaired differentiation of T cell subsets, and abnormal function of immune cells such as microglia in the central nervous system [4–8]. Notably, studies have observed downregulation of neuronal and synaptic function in ASD, coupled with an elevated neuroinflammatory response [9]. Persistent abnormalities in Treg cells function have also been reported in individuals with ASD [10, 11]. Consequently, immunotherapy has emerged as an avenue for the diagnosis and treatment.

Interleukin-2 (IL-2) plays a crucial role in enhancing immune responses by regulating T cells differentiation and promoting Treg cells proliferation. High dose IL-2 therapy has been shown to suppress tumor growth by promoting the proliferation of NK cells and CTLs in cancer patients [12]. In contrast, low dose IL-2 (LdIL-2) selectively targets and activates Treg cells, thereby helping to regulate inflammatory diseases [13–18]. For instance, in patients with systemic lupus erythematosus (SLE), LdIL-2 treatment significantly reduces disease activity by restoring the balance among Tfh, Th17, and Treg cells [19]. Similarly, studies have shown that Treg cells decrease while pro-inflammatory Th1 and Th17 cells increase in BTBR mice [20, 21]. Ahmad's research further demonstrated that modulating the Th17/Treg axis can improve ASD-like behaviors and neuroimmune function [20]. Alhosaini's work [22] corroborated these findings, showing that immune system restoration improved behavioral deficits in BTBR mice with

[1]The Second Affiliated Hospital of Kunming Medical University, Kunming, Yunnan, China. [2]Shanghai Institute of Immunology, Shanghai Jiao Tong University School of Medicine, Shanghai, China. [3]These authors contributed equally: Meng Li, Xiuying Kui. ✉email: binli@shsmu.edu.cn; caoxia@kmmu.edu.cn

Received: 2 April 2024 Revised: 7 August 2025 Accepted: 1 September 2025
Published online: 06 October 2025

ASD. Our previous study also identified the imbalance of Th/Treg cells as a potential diagnostic marker for ASD associated with immune dysfunction [23]. Collectively, these findings suggest that restoring immune balance could be an effective therapeutic approach for ASD in BTBR mice.

While immune therapies have shown promise in treating ASD, further investigation is needed to clarify the role of IL-2 in modulating ASD symptoms and to develop strategies for therapeutic modulation. In this study, we explored the effects of LdIL-2 on the balance between Treg cells and pro-inflammatory cells in BTBR mice with ASD traits. This preliminary investigation represents an important step toward the development of novel ASD therapies. Our findings may pave the way for identifying effective LdIL-2 treatments for ASD.

MATERIALS AND METHODS

Mice

BTBR $T^{+}Itpr3^{tf}$/J (BTBR) mice were purchased from The Jackson Laboratory and bred in-house at the Kunming Medical University animal facility. Animals were housed under strictly monitored specific, and opportunistic pathogen-free conditions. C57BL/6 mice were obtained from Beijing Huafukang Biotechnology Co., Ltd. All mice were male and aged 6–8 weeks at the time of each experiment. Because the proportion of boys with autism were significantly higher than girls [24]. Mice were allocated to control or experimental group randomly. All experimental protocols involving animal studies were approved by the Ethical Committee for Animal Studies of Kunming Medical University. The number of mice in different group were consulted other researches about autism using BTBR mice [24, 25].

Drug treatment

Recombinant human IL-2 (Quanqi, Shandong Quangang Pharmaceutical) was dissolved in 100 µl of sterile normal saline for injection (0.9% NaCl). BTBR mice in the treatment group were continuously injected with LdIL-2 subcutaneously (i.h.) injection for four courses, 7 days as a course at doses of 10,000 IU, 30,000 IU and 100,000 IU, with a one-day interval between each course [19, 26]. The control received subcutaneous injections of an equivalent volume of normal saline.

For Treg depletion, BTBR mice were intraperitoneally injected with 200 µg of purified anti-mouse CD25 antibody (PC61) (Biolegend). Control BTBR mice received 200 µg of purified control IgG1 (BioXCell). Treg depletion was conducted one day prior to, and on days 14 days and 28 days following, LdIL-2 treatment.

Three-chamber social test

The apparatus consisted of a 60 × 40 cm Plexiglas box divided into three interconnected chambers. The test was conducted in an isolated, soundproof room under dim lighting conditions. The animals were allowed access to each chamber through doors (12 × 6 cm) between the adjacent chambers.

Habituation phase. The experimental mice were placed in the central chamber, with an empty cage in the two side chambers, and were allowed to freely explore the apparatus for 10 m. The time spent by each mouse in the left and right chambers was recorded, mice showing an innate chamber preference were excluded from further testing. **Social Interaction Phase** The test mouse was directed to the center chamber, and an age- and strain-matched male stranger mouse (Stranger 1) was placed in a confinement cage in one of the side chambers. The test mice were allowed to explore all areas for 10 min. **Social Novelty Phase** The test mice were confined to the central chamber with the door closed for 10 min. A second unfamiliar, age- and strain-matched male mouse (Stranger 2) was then placed in the empty restraint cage in the opposite chamber, and the test mice were allowed to explore freely for another 10 min. The sniffing behavior and locomotor activity of the test mice were observed and recorded. The Social Approach Preference Index was calculated as follows: (Time spent sniffing Stranger 1-Time spent sniffing empty)/(Time spent sniffing Stranger 1+Time spent sniffing empty), and the Social Novelty Preference Index was calculated as follows: (Time spent sniffing Stranger 2-Time spent sniffing Stranger 1)/(Time spent sniffing Stranger 1+Time spent sniffing Stranger 2).

Self-grooming test

The test mouse was individually placed in a new test cage. After 10 min of habituation, the mouse's behavior was monitored for an additional 10 min using a video recorder. A trained observer, blinded to the treatment status of the test mouse, used a stopwatch to record the cumulative time spent grooming different body areas (face, head, or other body parts) as an indicator of repetitive stereotypic behavior.

Sniffing test

The test mouse and an unfamiliar mouse (age-, sex-, and strain-matched) were placed in a new test cage. Following a 10-min habituation period, the behavior of the mice was monitored for additional 10 min using video-recorder. A trained observer used a stopwatch to record the cumulative time the test mouse spent sniffing the other mouse's body by reviewing the video footage.

Marble-burying test

The apparatus used for the marble-burying test was a clean cage measuring 40 × 20 × 13 cm, filled with 5 cm of bedding. The bedding surface contained 20 clear glass marbles of 15 mm, arranged in a 4 × 5 grid pattern. Each mouse was placed in a corner of the cage that did not contain any marbles and was allowed a 10-min exploration period. After this period, the number of marbles that had been buried was counted. "Buried" was defined as 2/3 covered by bedding.

Open field test

The open field test apparatus consisted of a square white box of 40 × 40 × 30 cm, with the bottom divided into 16 small grids in a 4 × 4 pattern, where the central 4 grids constituted the central area. At the start of the experiment, the mouse was placed in the center of the apparatus, and its behavior was recorded by a camera for 10 min. At the end of each test, the apparatus was cleaned thoroughly with 75% alcohol. The total distance moved by the mice and the time spent in the central area were quantified using smartv3.0 behavioral analysis software.

Y-maze test

The experiment was divided into a training period and a testing period. The training period lasted four days, followed by the testing period on the fifth day.

Training period. The mice were deprived of water for 8–12 h before the experiment. Thirty minutes prior to the start of each training session, the mice were acclimated to the testing room and allowed to freely explore the Y-maze for 5 min. A green triangular piece of paper was affixed to the wall of the maze, except the starting arm, with 2% sucrose water placed beneath this marker. Each mouse underwent five training sessions per day, with the sequence of arms used for training varying across sessions. There was an interval of at least 10 min between each session for the same mouse. To prevent habituation, the arm sequence for the first training session of each day was different from that of the previous day. The card and sucrose water were consistently placed in the same position throughout the training period.

Testing period. Prior to testing, the mice were again deprived of water and the triangular paper markers were kept in place, but no sucrose water was provided. The mice were allowed to explore freely for 5 min, alternating between arms. The total time spent by each mouse exploring the arm with the card was recorded across two exploration procedures, and the proportion of the total time spent by the mice exploration sessions. The ratio of the time spent in the card arm to the total time spent in the non-main arms (with the starting arm considered the main arm) was calculated. At the conclusion of the experiment, the bottom of the maze was wiped with alcohol to eliminate any odors that could interfere with the experiment.

Preparation of mouse cells

BTBR and C57 mice were anesthetized with sodium pentobarbital before blood, spleens, and brains were removed aseptically. The collected blood was mixed with 3 ml of red blood cell lysis buffer and incubated for 15 min at room temperature. Following incubation, the cells were centrifuged at 400 × g for 5 min and then resuspended in RPMI-1640 medium. The resulting cell pellet constituted the peripheral blood single-cell suspension used for the experiment.

Spleen cells were isolated by grinding the tissue through a 200-mesh sieve in RPMI-1640 medium containing 10% FBS. The cells were then collected by centrifugation at 400× g for 5 min, resuspended in 3 ml of red blood cell lysis buffer, and incubated for 15 min at room temperature.

The mouse prefrontal cortex and hippocampus tissues were placed in a petri dish, cut into pieces, and mixed with 2 ml of collagenase / DNase solution. The tissue was incubated on a shaker at 37 °C for 30 min. After incubation, the solution was strained through a 200-mesh sieve and centrifuged at 300 g for 10 min. The resulting cell pellet was resuspended in 4 ml of cold 90% multifunctional separation solution (consisting of 90 ml Percoll and 10 ml 10 × HBSS). Next, 3 ml of 60% multifunctional separation solution (60 ml Percoll, 10 ml 10 × HBSS and 30 ml DEPC water), 30% multifunctional separation solution (30 ml Percoll, 10 ml 10 × HBSS, 60 ml DEPC water), and 3 ml 1 × HBSS were added sequentially. The cells were then subjected to gradient centrifugation at 450× g and 4 °C for 20 min (3 liters, 3 drops). The loose white cell layer was carefully collected, washed with 10 ml of 1 × HBSS, and centrifuged at 300× g at 4 °C for 10 min to collect the cells.

Flow cytometry

The cells were counted and stained for surface and intracellular markers following flow cytometry protocols. For Treg cells analysis, 2×10^6 cells from single-cell suspensions were fixed and permeabilized using 1 × fixation and permeabilization buffers (Biolegend). After washing with 1 × Permeabilization Buffer, the cells were surface-stained with CD3-PerCP, CD4-FITC, CD45-APC/FireTM750 (Biolegend), CD25-APC (BD), and Foxp3-PE (Invitrogen).

For Th1/Th2/Th17 cells analysis, 2×10^6 cells of single-cell suspension were cultured in RPMI-1640 medium containing 10% FBS and stimulated with 2 μl Cell Activation Cocktail (with Brefeldin A) (BioLegend)at 37 °C in 5% CO_2 for 5 h. Cells were stained for surface molecules (CD3e-APC, CD4-FITC) (Biolegend), fixed with Cold Fixation Buffer and permeabilized with Intracellular Staining Perm Wash Buffer and then intracellularly stained with IFN-γ-PE, IL-4-PE or IL-17A-PE (Biolegend).

For Tfh cells analysis, 2×10^6 cells from single-cell suspensions were surface stained with CD3-PerCP, CD4-FITC, CD45-APC / FireTM750, CXCR7-PE, CXCR5-APC and PD1-APC / FireTM750 (Biolegend).

For M1/M2 microglia analysis, 2×10^6 cells of single-cell suspensions were surface-stained with CD45-PerCP, CD11b-FITC, CD86-PE / Cyanine7 or CD206-PE / Cyanine7 (Biolegend).

Fluorescent real-time quantitative PCR

Total RNA was extracted from brain tissues using Eastep® Super (Promega), and quantified with NanoDrop (Thermo Scientific). cDNA was synthesized from total RNA using an RT kit (Promega), and RT-PCR was performed using NovoStart SYBR qPCR SuperMix Plus (Novoprotein) according to the manufacturer's instructions. The primers used were selected from NCBI, with the following sequences:

IL-6 forward (F): 5′-GTCCTTCCTACCCCAATTTCCA-3′;
reverse (R): 5′-GGAAATTGGGGTAGGAAGGA-3′;
IL-1β F: 5′-TGCCACCTTTTGACAGTGATG-3′
R: 5′-TGATGTGCTGCTGCGAGATT-3′;
TNF-α F: 5′-TAGCCCACGTCGTAGCAAAC-3′;
R: 5′-ACAAGGTACAACCCATCGGC-3′;
TGF-β F: 5′-GGAACACTGCTGAAAGGGGA-3′;
R: 5′-AGTAAATCCCGGAGGACCCA-3′;
Arg-1 F: 5′-AGGAAAGCTGGTCTGCTGGAA-3′;
R: 5′-AGATGCTTCCAACTGCCAGAC-3′;
β-actin F: 5′-CTGAGAGGGAAATCGTGCGT-3′;
R: 5′-CCACAGGATTCCATACCCAAGA-3′.

RT-PCR data were analyzed using the relative and comparative gene expression (ΔΔCT) method. The results were presented as fold changes in gene expression, normalized to the housekeeping gene β-actin.

Immunofluorescence

Mice were anesthetized with sodium pentobarbital and perfused with PBS, followed by 4% paraformaldehyde. The brains were dissected, dehydrated in a 30% sucrose solution, frozen, and then sectioned into 25-μm coronal sections.

Brain sections were transferred to glass slides, rewarmed, and washed with 0.3% PBST (0.3% TritonX-100 in PBS) for 15 min, The sections were then blocked with 3% goat serum for 1 h at room temperature, incubated with primary antibody overnight at 4 °C, washed in PBST, and incubated with the appropriate secondary antibody for 1 hour at 37 °C. The following antibodies were used: Mouse anti-NeuN (Abcam, ab104224; 1:1000), Rabbit anti-Iba1 (Abcam, ab178846; 1:4000), Alexa Fluor™ 568 goat anti-Rabbit IgG (H + L) (Invitrogen, 1892091; 1:1000), Alexa Fluor 488 anti-mouse IgG (Cell Signaling, #4408S; 1:1000). Cell nuclei were stained with DAPI (Abcam, ab104139). Immunofluorescence images were captured with a fluorescence microscope (Olympus). Four random shots were taken in each brain region and counted. The mean value was then used to represent the number of cells in that part of the mouse for statistical analysis. Analysis and counting were performed using ImageJ.

Statistics

The Kolmogorov-Smirnov test was employed to assess the normality of the data distribution. Subsequently, an independent samples t-test was conducted to compare the index differences between the normal group, and a one-way ANOVA was utilized to compare the index differences among the intervention groups. Statistical analyses were performed using SPSS v.20.0. Plots were generated with GraphPad Prism v8.0.2.263. A P value of <0.05 was considered statistically significant.

RESULTS

LdIL-2 improves autism-like behavior in autistic BTBR mice

We investigated the effects of different courses and doses of low-dose IL-2 (LdIL-2) on social approach preference and self-grooming behavior in BTBR mice. The behaviors of BTBR mice have improved significantly upto four courses treatment (Fig. 1B). And it also improved in the group which were treated with 30,000 IU of LdIL-2 (Fig. 1C). Based on these findings, we selected the four courses and 30,000 IU dosage for subsequent experiments aimed at treating ASD-related behaviors in BTBR mice. To further assess the effects of LdIL-2, we conducted behavioral evaluations focusing on social behavior, repetitive stereotypic behavior, and anxiety-related behavior in BTBR mice. In the three-chamber social test, BTBR mice exhibited significantly lower social engagement compared to C57 mice. However, after LdIL-2 treatment, the social approach preference index in BTBR mice was significantly higher than in the untreated control group. Despite this improvement, no significant changes were observed in their social novelty preference index (Fig. 1D, E). In addition, LdIL-2 treatment significantly reduced self-grooming and increased sniffing behavior in BTBR mice. (Fig. 1F, G). In the marble burying test, which assesses repetitive and anxiety-like behaviors, we observed a decrease in marble-burying behavior following LdIL-2 treatment (Fig. 1H). We also evaluated spontaneous exploratory behavior using the open field test. While the overall activity levels of BTBR mice were not significantly different from those of C57 mice, BTBR mice spent less time in the central region of the arena compared to the normal mice. Unfortunately, LdIL-2 treatment did not result in a significant improvement in this behavior (Fig. 1I). Lastly, in the Y-maze test, which assesses working memory and cognitive flexibility, the time spent in the training arm (card arm) was significantly increased in BTBR mice after LdIL-2 treatment (Fig. 1J). In conclusion, consistent with previous studies, we observed distinctive autism-like behaviors in BTBR mice. Importantly, our study demonstrated that LdIL-2 treatment significantly ameliorated these abnormal behaviors, particularly in social and stereotyped behaviors.

LdIL-2 modulates Th/Treg balance to ameliorate peripheral immune imbalance in BTBR mice

In this study, we utilized flow cytometry to compare Treg cell levels in the peripheral blood of BTBR mice and C57 mice, as well as to assess the effects of LdIL-2 treatment on these levels. BTBR mice exhibited a clear peripheral immune imbalance compared to normal C57 mice, characterized by a lower proportion of Treg cells in both the peripheral blood and spleen (Fig. 2A, B), along with elevated Th17/Treg, Th1/Treg, and Tfh/Treg ratios in the spleen (Fig. 2C–E). Additionally, the anti-inflammatory cytokine TGF-β was found to be significantly reduced in the peripheral blood of BTBR

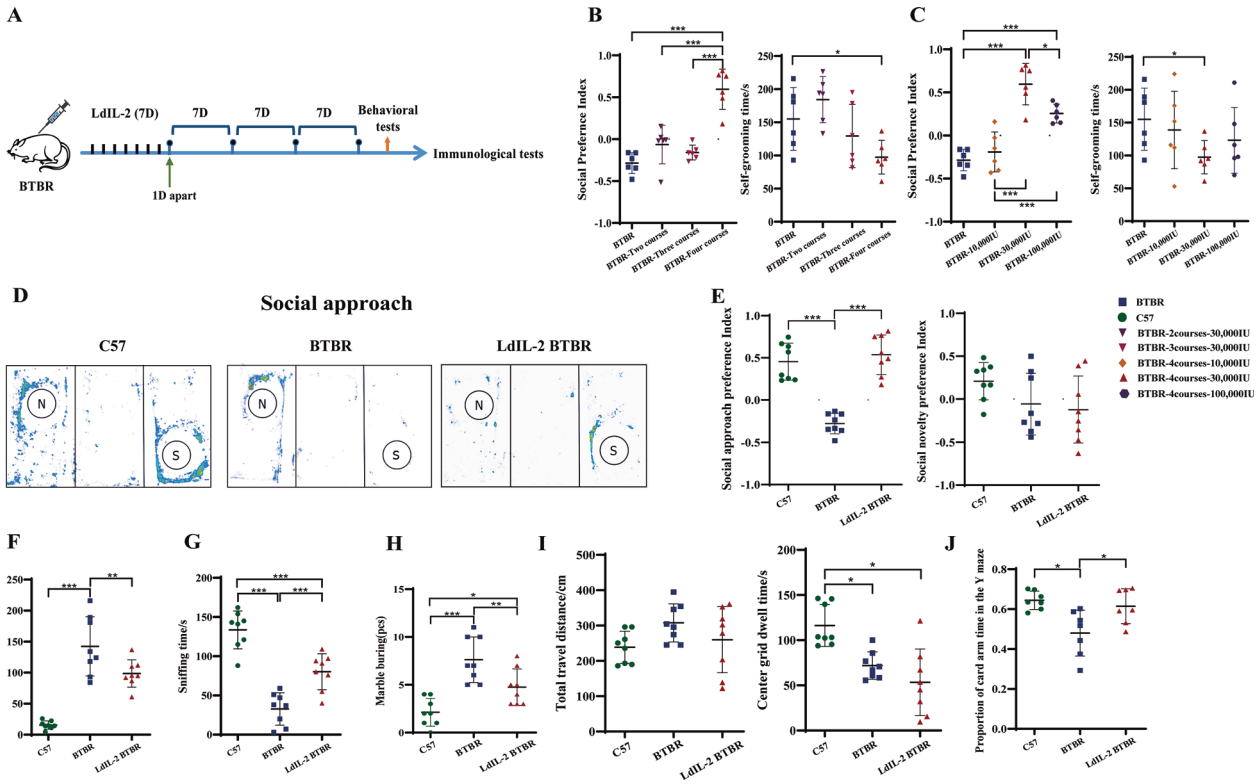

Fig. 1 The changes of autism-like behaviors before and after LdIL-2 treatment in mice. (C57 was used as the healthy control) **A** LdIL-2 treatment prescription; **B** different courses of LdIL-2 to BTBR mice, n = 6; **C** different dosages of IL-2 to BTBR mice, n = 6; **D** three-chamber social test (N: null, S: stranger mouse); **E** compare of social approach preference index and social novelty preference index in C57, before and after LdIL-2 treatment BTBR mice, n = 8; **F** self-grooming time, n = 8; **G** sniffing time, n = 8; **H** marble burying, n = 8; **I** total travel distance and center grid dwell time, n = 8; **J** proportion of card arm time in the Y maze, n = 7. ***P < 0.001, **P < 0.01, *P < 0.05.

mice compared to C57 controls (Fig. 2F). Following LdIL-2 treatment, the proportion of Treg cells in the peripheral blood and spleen of BTBR mice significantly increased (Fig. 2A, B). Moreover, the treatment effectively ameliorated the immune imbalance in BTBR mice, as evidenced by a reduction in Th17/Treg and Tfh/Treg ratios in the spleen (Fig. 2C–E). The levels of the anti-inflammatory cytokine TGF-β in plasma also increased post-treatment (Fig. 2F). Interestingly, despite these immunomodulatory effects, no significant changes in IL-2 levels were detected in treated mice.

LdIL-2 ameliorates neuroinflammation in BTBR mice

BTBR mice exhibit persistent immune imbalance when compared to C57 mice, including elevated levels of pro-inflammatory cytokines such as IL-1β, TNF-α and IL-6, as well as chemokines like MCP-1. These mice also display prominent M1 polarization and adaptive immune response disorders [27]. In this study, we further observed reduced levels of Treg cells in both the hippocampus and cortex of BTBR mice compared to C57 mice (Fig. 3A, B). Moreover, the levels of pro-inflammatory cytokines, including IL-1β, IL-6, and TNF-α, were significantly elevated in the cortex of BTBR mice, and similarly, IL-1β and IL-6 were higher in the hippocampus of BTBR mice compared to C57 mice. In contrast, the levels of anti-inflammatory cytokines, such as TGF-β and arginase-1 (Arg-1), were notably lower in the cortex and hippocampus of BTBR mice than in C57 mice (Fig. 3C, D). Besides, we visually observed a high increase in the number of microglia marked by Iba1 both in hippocampus and cortex of BTBR. After LdIL-2 treatment, the number of microglia decreased in these two regions (Fig. 3E–H). As the macrophage of neurol immune system, microglia involved the immune regulation by proliferation, activation and polarization. Immunofluorescence analysis also revealed a reduced number of NeuN+ neurons in the cortex and hippocampus of BTBR mice compared to C57 mice, although there was no significant difference observed in the CA3 region of the hippocampus (Fig. 3I–L). After LdIL-2 treatment, we observed an increase in Treg cell proportions in the hippocampus, along with a decrease in IL-1β, IL-6, and TNF-α levels. Simultaneously, the levels of anti-inflammatory markers TGF-β and Arg-1 were significantly increased in both the cortex and hippocampus of BTBR mice (Fig. 3C, D). Additionally, the number of NeuN+ neurons in the cortex showed a marked increase following LdIL-2 treatment which exerts a significant ameliorative effect on neuroinflammation in the prefrontal cortex of BTBR mice (Fig. 3I–L).

To assess whether the neuroimmunomodulatory effects of LdIL-2 in autistic BTBR mice were associated with microglia polarization, we analyzed the expression levels of CD45, CD11b, CD86, and CD206 in the cortex and hippocampus using flow cytometry. These markers were used to investigate the impact of LdIL-2 on the phenotypic transformation of microglia. Our findings revealed a significant reduction in the M1/M2 microglia ratio in both the cortex and hippocampus of BTBR mice following LdIL-2 treatment. This indicates that LdIL-2 promotes the maintenance of a dynamic balance between M1 and M2 microglia in the cortex and hippocampus of autistic BTBR mice (Fig. 3M, N). In addition, we observed alterations in protein levels within the cerebrospinal fluid of BTBR mice before and after LdIL-2 treatment. Notably, several neuroinflammation-related proteins, such as Filamin-A, were significantly reduced following LdIL-2 administration (Fig. 3O).

PC61 depletion of Treg cells attenuates the therapeutic effect of LdIL-2 on BTBR mice

To assess the role of Treg cells in the therapeutic efficacy of LdIL-2 in BTBR mice, we administered an anti-CD25 antibody (PC61) via

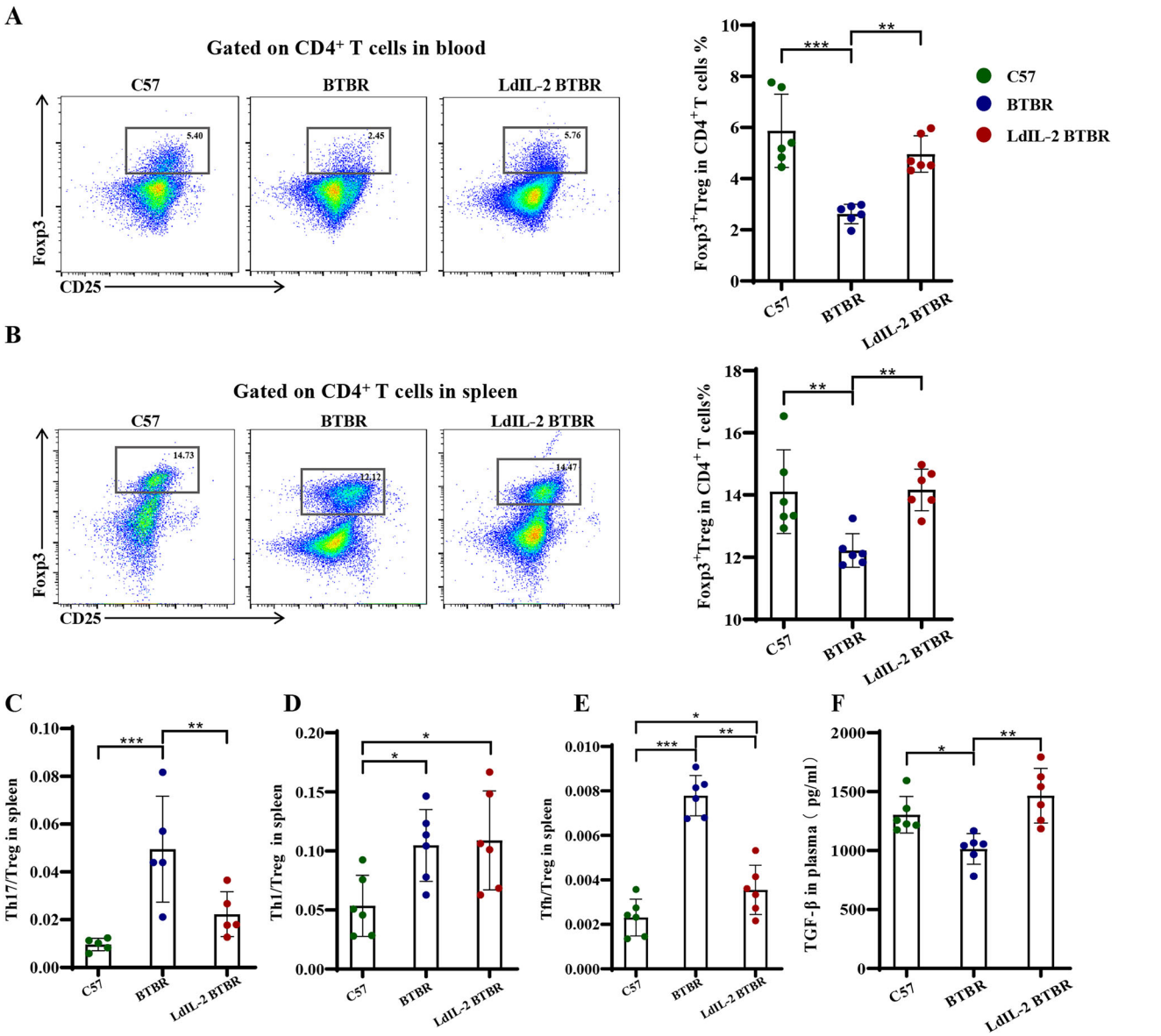

Fig. 2 Levels of T cell subsets and immune balance in peripheral of BTBR mice based on Treg cells assistance. A $CD4^+Foxp3^+$ Treg cells proportion in $CD4^+$T cells of peripheral blood in mice, n = 6; **B** $CD4^+Foxp3^+$ Treg cells proportion in $CD4^+$T cells of spleen in mice, n = 6; **C** Tfh/Treg in $CD4^+$T cells of spleen in mice, n = 6; **D**: Th17/Treg in $CD4^+$T cells of spleen in mice, n = 6; **E**: Th1/Treg, in $CD4^+$T cells of spleen in mice, n = 6; **F**: level of TGF-β in mouse plasma, n = 6. ***P < 0.001, **P < 0.01, *P < 0.05.

intraperitoneal injection prior to LdIL-2 treatment (Fig. 4A). One day after PC61 administration, Treg cells in the peripheral blood and spleen were markedly depleted (Fig. 4B). Compared with the IgG1+LdIL-2-treated group, the PC61 intervention resulted in a significant reduction of Treg cell levels in both the peripheral blood and spleen (Fig. 4C, D), accompanied by a decrease in TGF-β levels (Fig. 4E). This depletion negated the primary effect of LdIL-2, namely, the elevation in Treg cell numbers. Notably, the behavioral improvements observed in BTBR mice treated with LdIL-2 were significantly diminished when Treg cells were depleted by PC61. The social approach preference index in the PC61+LdIL-2 group showed minimal change from baseline when compared with the BTBR control group (Fig. 4F). Furthermore, PC61 treatment abolished the LdIL-2-induced improvements in self-grooming behavior, sniffing time, and marble-burying activity, rendering them comparable to those of untreated BTBR mice (Fig. 4G–I). Besides, compared with IgG1+LdIL-2-treatment, pro-inflammatory cytokines like IL-1β, IL-6, TNF-α and iNOS stayed at high levels and TGF-β at a low level in cortex and hippocampus of BTBR mice in PC61+LdIL-2 group. The results indicated that PC61 which inhibited Treg cells restrained the effects of LdIL-2. In the PC61+LdIL-2 group, inflammation of neuron was more serious comparing the IgG1+LdIL-2. Obviously, the LdIL-2 increased Treg cells level and immunologic function at the same time (Fig. 4J, K).

DISCUSSION

Numerous studies have provided evidence of immune dysfunction in ASD patients, including the dysregulation of cytokines and immune cells [8]. Previous research has explored various immune-based treatments for ASD and demonstrated certain therapeutic effects. Immunotherapy methods such as steroids, stem cells, and immunoglobulins have shown improvements in some of the disordered behaviors associated with ASD, including anxiety, self-aggression, irritability, sleep disturbances, and hyperactivity. Regulating immune dysfunction in children with ASD is necessary

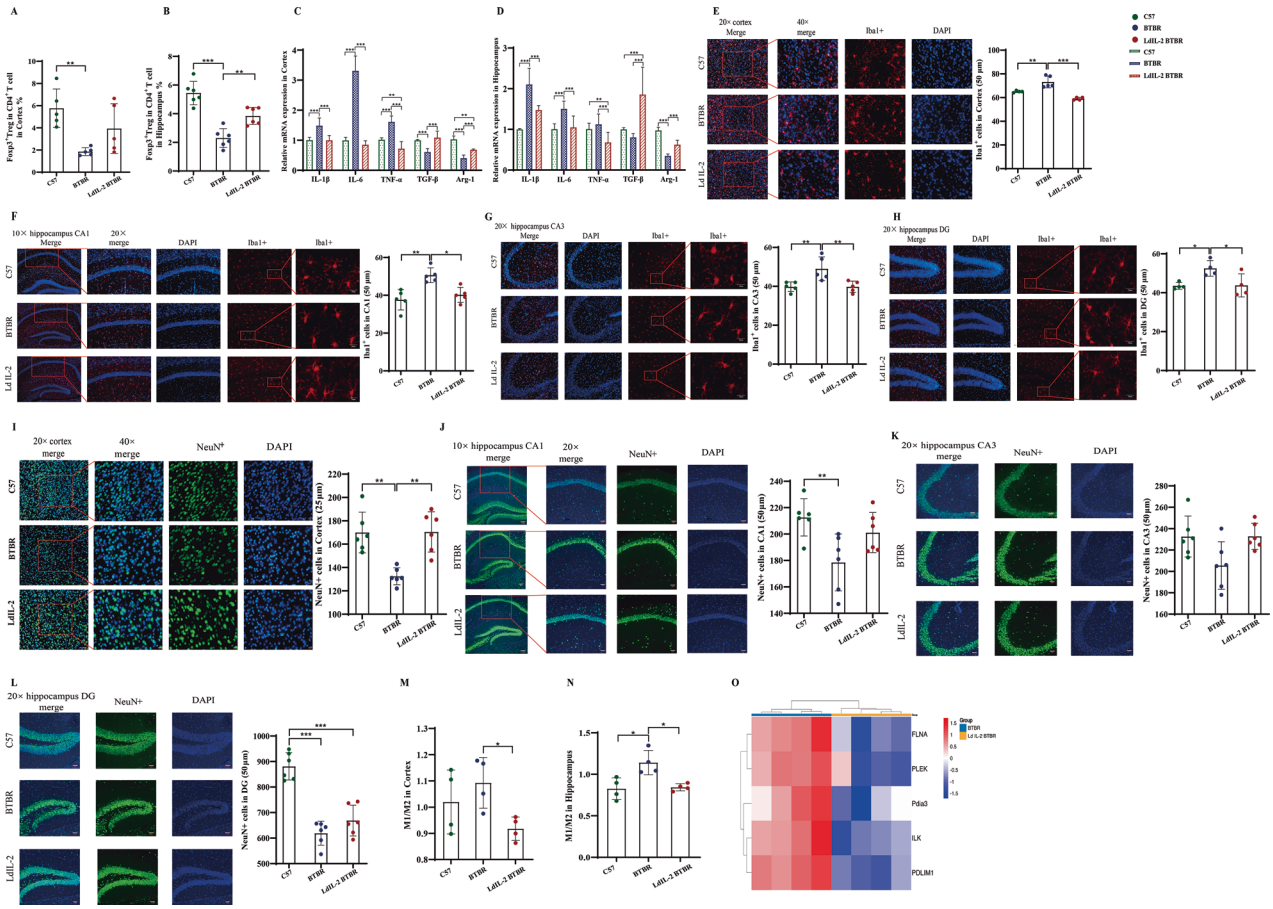

Fig. 3 Neuroinflammatory changes in BTBR mice after LdIL-2 treatment. A proportion of Treg cells in the cortex of BTBR mice after LdIL-2 treatment, n = 5; **B** proportion of Treg cells in the hippocampus of BTBR mice after LdIL-2 treatment, n = 5; **C** expressions of cytokines in the cortex of BTBR mice after LdIL-2 treatment; **D** expressions of cytokines in the hippocampus of BTBR mice after LdIL-2 treatment; **E** immunofluorescence of Iba1 in cortex of BTBR after LdIL-2 treatment, n = 4–5; **F** immunofluorescence of Iba1 in hippocampus CA1 of BTBR after LdIL-2 treatment, n = 5; **G** immunofluorescence of Iba1 in hippocampus CA3 of BTBR after LdIL-2 treatment, n = 5; **H** immunofluorescence of Iba1 in hippocampus DG of BTBR after LdIL-2 treatment, n = 4; **I** immunofluorescence of NeuN in cortex of BTBR after LdIL-2 treatment, n = 6; **J** immunofluorescence of NeuN in hippocampus CA1 of BTBR after LdIL-2 treatment, n = 6; **K** immunofluorescence of NeuN in hippocampus CA3 of BTBR after LdIL-2 treatment, n = 6; **L** immunofluorescence of NeuN in hippocampus DG of BTBR after LdIL-2 treatment, n = 6; **M** ratio of M1/M2 microglia in cortex of BTBR after LdIL-2 treatment, n = 4; **N** ratio of M1/M2 microglia in hippocampus of BTBR after LdIL-2 treatment, n = 4; **O** changes in the expression of inflammatory proteins in cerebrospinal fluid of BTBR mice. ***P < 0.001, **P < 0.01, *P < 0.05.

to improve core symptoms. For instance, Treg cells transfer has been shown to reverse the ASD phenotype [28]. However, existing research is not yet sufficient to definitively establish the efficacy of these immune treatments in addressing the core symptoms of ASD. Consequently, further exploration of targeted immunotherapy approaches is warranted to effectively address these core symptoms.

It has been observed that LdIL-2 preferentially stimulates Treg cells when administered at doses between 15,000 to 30,000 IU daily [29, 30]. Additionally, regulating the Th1, Tfh, and Th17 to Treg cell ratios has proven vital in addressing immune-related diseases [31, 32]. In a study led by Jing He [19, 26] on systemic lupus erythematosus (SLE), disease activity was significantly reduced through LdIL-2 treatment by modulating the relative proportions of Tfh, Th17, and Treg cells. Other studies, including our own [23, 27, 33], have shown that inflammatory cytokines and $CD4^+$ and $CD8^+$T cells in immune organs and peripheral blood, along with various immune cells in the brains of BTBR mice, are disordered at different levels compared to C57 mice. Notably, several studies have demonstrated a reduction in Treg cells, while Th1 and Th17 cells associated with inflammation were elevated in BTBR mice [20]. In our study, increased Th/Treg ratios and pro-inflammatory cytokines in BTBR mice further supported the theory of immune dysregulation in ASD. Following LdIL-2 treatment, these imbalances were restored to levels closer to those seen in C57 mice, illustrating that immune therapy may effectively reverse neuroinflammation in ASD.

Given the reduction of Treg cells observed in the immune system of BTBR mice, we used three specific doses of IL-2 in a four-course treatment regimen (Fig. 1B, C) according to the definition of LdIL-2 [29, 30]. The selected IL-2 doses were based on the findings from studies on SLE by Zhanguo Li [19]. In our experiments, IL-2 was administered at 10,000 IU, 30,000 IU, and 100,000 IU, each given for four courses. Although the 100,000 IU dose showed certain behavioral benefits, it also resulted in increased activation of effector T cells, including Th2 cells, raising concerns about potential immune overstimulation at higher doses. In contrast, the 30,000 IU dose consistently improved behavioral outcomes and promoted immune balance without triggering adverse immune activation. Based on these findings, we identified 30,000 IU as the most suitable dose for subsequent experiments. Although we did not further investigate the effects of varying treatment durations with the 100,000 IU dose, future studies are needed to systematically examine the relationship

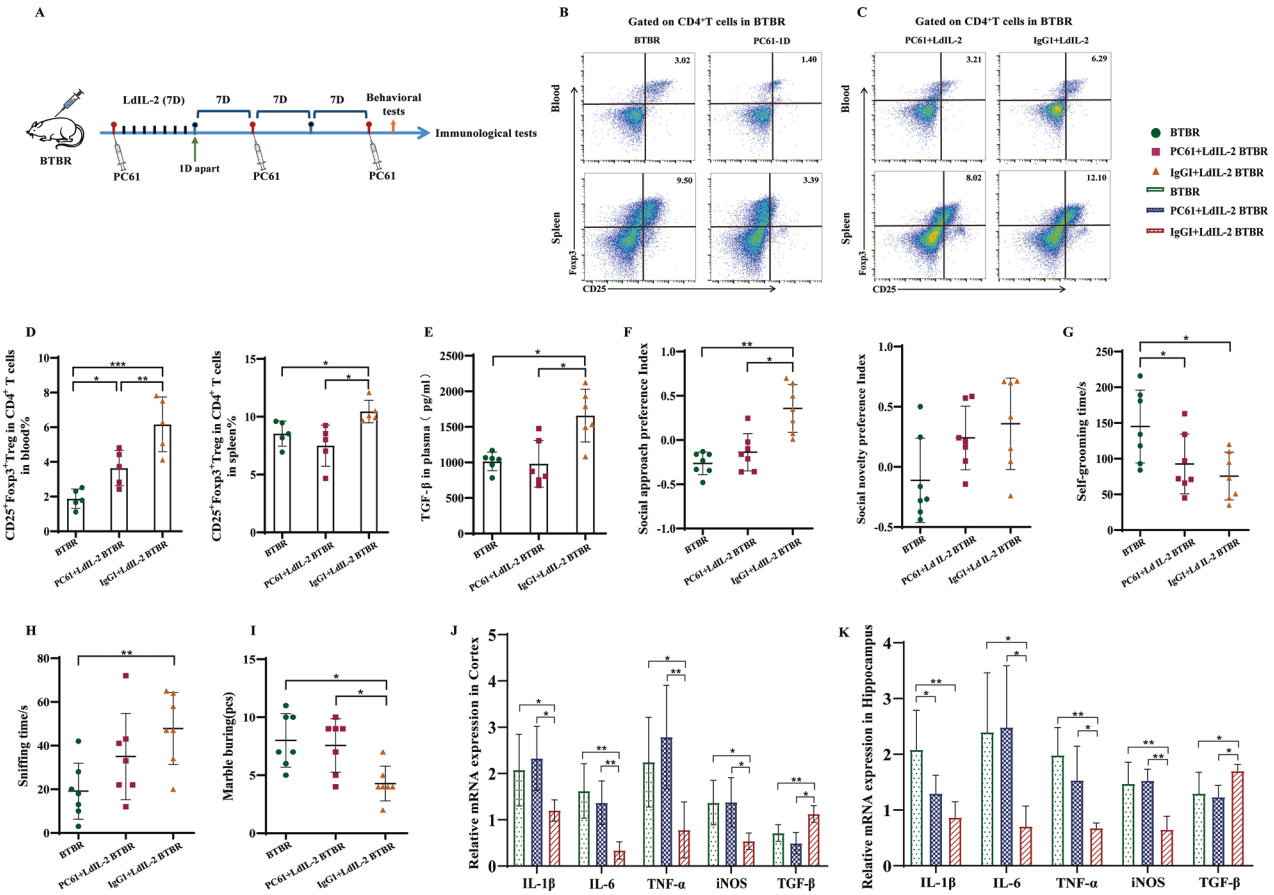

Fig. 4 Effect of PC61 intervention on LdIL-2 treatment outcome. A PC61 and LdIL-2 treatment prescription; **B** flow cytometry images of Treg cells in peripheral blood and spleen of BTBR mice one day after PC61 intervention; **C** flow cytometry images of Treg cells in peripheral blood and spleen of BTBR mice after PC61 intervention, IgG1 was used as control of PC61 treatment; **D** proportion of Treg cells in peripheral blood and spleen of BTBR after PC61 and LdIL-2 treatment, n = 5; **E** level of TGF-β in plasma, n = 6; **F** compare of social approach preference index and social novelty preference index, n = 7; **G** self-grooming time, n = 7; **H** sniffing time, n = 7; **I** marble burying, n = 7; **J** expressions of cytokines in the cortex of BTBR mice after PC61 and LdIL-2 treatment; **K** expressions of cytokines in the hippocampus of BTBR mice after PC61 and LdIL-2 treatment. ***P < 0.001, **P < 0.01, *P < 0.05.

between IL-2 dosage, treatment course, and therapeutic efficacy in ASD models. In the autistic behavior tests for BTBR mice, social approach preference was used to assess sociability, while self-grooming was used to evaluate repetitive behavior [34]. Repetitive and stereotyped behaviors, such as self-grooming and marble-burying, were significantly improved after LdIL-2 therapy [35]. The observed changes in Treg cell proportion in both the peripheral blood and the central nervous system indicated that LdIL-2 effectively regulated immune function. IL-2 upregulated FOXP3 expression in Treg cells through STAT5 activation [36], while reductions in Th17/Treg and Tfh/Treg ratios also reflected LdIL-2's role in restoring immune balance. Additionally, TGF-β, a key anti-inflammatory cytokine mediating both Th17 and Treg differentiation, was upregulated [37]. Our tests on other helper T cells, including Th1, revealed no statistically significant changes (Fig. 2D), highlighting the dynamic nature of T cell subpopulations. The imbalance between Th17 and Treg cells has been implicated in the pathogenesis of autoimmune disease such as SLE [38, 39]. Studies have shown that in the presence of IL-6 or IL-21 (along with TGF-β), naïve $CD4^+$T cells differentiate into Th17 cells, while in the absence of pro-inflammatory cytokines, they differentiate into Treg cells [40]. In our study, the elevation of TGF-β indicated that LdIL-2 regulated inflammation in the peripheral immune system of BTBR mice. Further analysis of T cell subsets and cytokines in the cortex and hippocampus showed similar effects. Additionally, the Y maze test, which assesses learning and memory formation [41], demonstrated that LdIL-2 treatment improved cognitive and memory functions in BTBR mice. These findings suggest that LdIL-2 not only modulates neuroinflammation but also promotes a balanced pro- and anti-inflammation activity in the central nervous system of BTBR mice.

Furthermore, IL-2 was shown to regulate the immune system in the brains of BTBR mice. Substantial research on neuroinflammation suggests that T cells interact with microglia to suppress inflammation by releasing cytokines and modulating microglia phenotypes [42]. Our study revealed that as Treg cells level improved and Th/Treg ratios balanced in the periphery, pro-inflammatory cytokines decreased, anti-inflammatory cytokines increased, and the M1/M2 microglia ratio stabilized in both the cortex and hippocampus following LdIL-2 treatment. This provides strong evidence that LdIL-2 treatment effectively regulates microglia activity and reduces neuroinflammation in BTBR mice. Our findings also suggest that LdIL-2 treatment may promote neuronal maturation in the cortex of BTBR mice, as indicated by NeuN expression. Concurrently, LdIL-2 effectively reversed immune dysregulation and neuroinflammatory responses observed in these brain regions. These results suggest that neuroinflammation may represent a critical factor in impaired neuronal maturation in the BTBR mice model. Given the established immunomodulatory properties of LdIL-2, its capacity to suppress neuroinflammation might play a pivotal role in maintaining neuronal development. Therefore, we propose that

LdIL-2 may exert a neuroprotective role in BTBR mice by restoring immune balance and mitigating inflammatory processes, ultimately promoting neuronal maturation in the cortex. However, individual differences in BTBR mice suggest that IL-2 may not be the sole regulatory factor for neuronal damage. Given the observed improvements in both behavioral and inflammatory parameters in the peripheral and central nervous systems, we speculate that LdIL-2 may balance the immune system to regulate ASD-related behaviors. To our knowledge, this study is the first to provide evidence of the safety and efficacy of LdIL-2 (30,000 IU) in alleviating ASD symptoms. This novel intervention demonstrated the ability to ameliorate autism-related manifestations by fine-tuning the Th17/Treg and Tfh/Treg balance in BTBR mice. Additionally, changes in protein levels in cerebrospinal fluid, including a reduction in immune-related proteins like Filamin-A, were observed after LdIL-2 treatment [43]. Moreover, the mTOR pathway, which regulates cell growth and survival in response to nutrients, particularly neuron recovery and synaptic plasticity, was identified as a key factor in ASD [44]. The PI3K/Akt/mTOR pathway was also implicated in improving social interaction, neural development, and other ASD symptoms [45]. We are continuing to explore these neural pathways in ongoing research, with the goal of achieving more robust therapeutic effects.

Considering the significant changes in core ASD behaviors and T cell subsets following LdIL-2 treatment, we further investigated whether Treg cells play the most critical role in ameliorating ASD symptoms. To do so, we administered LdIL-2 after depleting Treg cells in the blood and spleen of BTBR mice using PC61, an anti-CD25 antibody that achieves Treg cells depletion via intraperitoneal injection [46]. Our findings indicated that behavioral and immune improvements in BTBR mice treated with PC61+LdIL-2 were minimal compared to the control group (IgG1+LdIL-2). Treg depletion by PC61 was only partially effective, as the remaining Treg cells still retained some regulatory function. This suggests that while Treg cells play a crucial role in the therapeutic effects of LdIL-2, other factors may also contribute to the regulation of ASD. Nonetheless, Treg cells remain key regulators of immune dysfunction in ASD.

This study has some limitations. It represents a preliminary investigation based on a mouse model. We anticipate conducting a randomized, double-blind, placebo-controlled clinical trial to comprehensively evaluate the safety and efficacy of LdIL-2 in human subjects. Furthermore, additional research into the specific mechanisms underlying LdIL-2's effects on ASD is warranted.

CONCLUSION

This study clearly demonstrates that LdIL-2 can ameliorate behavioral disturbances associated with ASD, particularly core symptoms such as social communication impairments and stereotyped behaviors. LdIL-2 exerts its effects by modulating immune balance in both the peripheral and central nervous systems of BTBR mice. This study offers compelling evidence that this therapy holds promise as a safe and effective treatment for ASD.

DATA AVAILABILITY

The original contributions presented in the study are included in the article. Further reasonable inquiries can be directed to the corresponding author.

REFERENCES

1. Aishworiya R, Valica T, Hagerman R, Restrepo B. An update on psychopharmacological treatment of autism spectrum disorder. Neurotherapeutics. 2022;19:248–62.
2. Tian J, Gao X, Yang L. Repetitive restricted behaviors in autism spectrum disorder: from mechanism to development of therapeutics. Front Neurosci. 2022;16:780407.
3. Canitano R, Palumbi R. Excitation/Inhibition modulators in autism spectrum disorder: current clinical research. Front Neurosci. 2021;15:753274.
4. Xu ZX, Kim GH, Tan JW, Riso AE, Sun Y, Xu EY, et al. Elevated protein synthesis in microglia causes autism-like synaptic and behavioral aberrations. Nat Commun. 2020;11:1797.
5. Ashwood P, Krakowiak P, Hertz-Picciotto I, Hansen R, Pessah I, Van de Water J. Elevated plasma cytokines in autism spectrum disorders provide evidence of immune dysfunction and are associated with impaired behavioral outcome. Brain Behav Immun. 2011;25:40–45.
6. Careaga M, Rogers S, Hansen RL, Amaral DG, Van de Water J, Ashwood P. Immune endophenotypes in children with autism spectrum disorder. Biol Psychiatry. 2017;81:434–41.
7. Honarmand Tamizkar K, Badrlou E, Aslani T, Brand S, Arsang-Jang S, Ghafouri-Fard S, et al. Dysregulation of NF-κB-associated lncrnas in autism spectrum disorder. Front Mol Neurosci. 2021;14:747785.
8. Hughes HK, Moreno RJ, Ashwood P. innate immune dysfunction and neuroinflammation in autism spectrum disorder (ASD). Brain Behav Immun. 2023;108:245–54.
9. Zhang P, Omanska A, Ander BP, Gandal MJ, Stamova B, Schumann CM. Neuron-specific transcriptomic signatures indicate neuroinflammation and altered neuronal activity in ASD temporal cortex. Proc Natl Acad Sci USA. 2023;120:e2206758120.
10. Akbari M, Eghtedarian R, Hussen BM, Eslami S, Taheri M, Neishabouri SM, et al. Assessment of expression of regulatory T cell differentiation genes in Autism Spectrum Disorder. Front Mol Neurosci. 2022;15:939224.
11. De Giacomo A, Gargano CD, Simone M, Petruzzelli MG, Pedaci C, Giambersio D, et al. B and T Immunoregulation: a new insight of B regulatory lymphocytes in Autism Spectrum Disorder. Front Neurosci. 2021;15:732611.
12. Boyman O, Kovar M, Rubinstein MP, Surh CD, Sprent J. Selective stimulation of T cell subsets with antibody-cytokine immune complexes. Science. 2006;311:1924–7.
13. Tahvildari M, Dana R. Low-Dose IL-2 therapy in transplantation, autoimmunity, and inflammatory diseases. J Immunol. 2019;203:2749–55.
14. Hartemann A, Bensimon G, Payan CA, Jacqueminet S, Bourron O, Nicolas N, et al. Low-dose interleukin 2 in patients with type 1 diabetes: a phase 1/2 randomised, double-blind, placebo-controlled trial. Lancet Diabetes Endocrinol. 2013;1:295–305.
15. Ballesteros-Tato A, Papillion A. Mechanisms of action of low-dose IL-2 restoration therapies in SLE. Curr Opin Immunol. 2019;61:39–45.
16. von Spee-Mayer C, Siegert E, Abdirama D, Rose A, Klaus A, Alexander T, et al. Low-dose interleukin-2 selectively corrects regulatory T cell defects in patients with systemic lupus erythematosus. Ann Rheum Dis. 2016;75:1407–15.
17. Yan J-J, Lee J-G, Jang JY, Koo TY, Ahn C, Yang J. IL-2/anti-IL-2 complexes ameliorate lupus nephritis by expansion of CD4+CD25+Foxp3+ regulatory T cells. Kidney Int. 2017;91:603–15.
18. Yokoyama Y, Iwasaki T, Kitano S, Satake A, Nomura S, Furukawa T, et al. IL-2-Anti-IL-2 monoclonal antibody immune complexes inhibit collagen-induced arthritis by augmenting regulatory T cell functions. J Immunol. 2018;201:1899–906.
19. He J, Zhang X, Wei Y, Sun X, Chen Y, Deng J, et al. Low-dose interleukin-2 treatment selectively modulates CD4(+) T cell subsets in patients with systemic lupus erythematosus. Nat Med. 2016;22:991–3.
20. Ahmad SF, Nadeem A, Ansari MA, Bakheet SA, Alshammari MA, Attia SM. The PPARδ agonist GW0742 restores neuroimmune function by regulating Tim-3 and Th17/Treg-related signaling in the BTBR autistic mouse model. Neurochem Int. 2018;120:251–61.
21. Ahmad SF, Ansari MA, Nadeem A, Bakheet SA, Alshammari MA, Khan MR, et al. S3I-201, a selective Stat3 inhibitor, restores neuroimmune function through upregulation of Treg signaling in autistic BTBR T+ Itpr3tf/J mice. Cell Signal. 2018;52:127–36.
22. Alhosaini K, Ansari MA, Nadeem A, Bakheet SA, Attia SM, Alhazzani K, et al. 5-Aminoisoquinolinone, a PARP-1 inhibitor, ameliorates immune abnormalities through upregulation of anti-inflammatory and downregulation of inflammatory parameters in T Cells of BTBR mouse model of autism. Brain Sci. 2021;11:249.
23. Nie Z-Q, Han D, Zhang K, Li M, Kwon H-K, Im S-H, et al. TH1/Treg ratio may be a marker of autism in children with immune dysfunction. Res Autism Spectr Disord. 2023;101:102085.
24. Bove M, Palmieri MA, Santoro M, Agosti LP, Gaetani S, Romano A, et al. Amygdalar neurotransmission alterations in the BTBR mice model of idiopathic autism. Transl Psychiatry. 2024;14:193.
25. Matrisciano F, Locci V, Dong E, Nicoletti F, Guidotti A, Grayson DR. Altered expression and in vivo activity of mGlu5 variant a receptors in the striatum of BTBR mice: novel insights into the pathophysiology of adult idiopathic forms of Autism Spectrum Disorders. Curr Neuropharmacol. 2022;20:2354–68.

26. He J, Zhang R, Shao M, Zhao X, Miao M, Chen J, et al. Efficacy and safety of low-dose IL-2 in the treatment of systemic lupus erythematosus: a randomised, double-blind, placebo-controlled trial. Ann Rheum Dis. 2020;79:141–9.
27. Careaga M, Schwartzer J, Ashwood P. Inflammatory profiles in the BTBR mouse: how relevant are they to autism spectrum disorders? Brain Behav Immun. 2015;43:11–16.
28. Xu Z, Zhang X, Chang H, Kong Y, Ni Y, Liu R, et al. Rescue of maternal immune activation-induced behavioral abnormalities in adult mouse offspring by pathogen-activated maternal T(reg) cells. Nat Neurosci. 2021;24:818–30.
29. Klatzmann D, Abbas AK. The promise of low-dose interleukin-2 therapy for autoimmune and inflammatory diseases. Nat Rev Immunol. 2015;15:283–94.
30. Arenas-Ramirez N, Woytschak J, Boyman O. Interleukin-2: biology, design and application. Trends Immunol. 2015;36:763–77.
31. Luz-Crawford P, Kurte M, Bravo-Alegría J, Contreras R, Nova-Lamperti E, Tejedor G, et al. Mesenchymal stem cells generate a CD4+CD25+Foxp3+ regulatory T cell population during the differentiation process of Th1 and Th17 cells. Stem Cell Res Ther. 2013;4:65.
32. Yan J-B, Luo M-M, Chen Z-Y, He B-H. The function and role of the Th17/Treg cell balance in inflammatory Bowel Disease. J Immunol Res. 2020;2020:8813558.
33. De Simone R, Butera A, Armida M, Pezzola A, Boirivant M, Potenza RL, et al. Beneficial effects of fingolimod on social interaction, CNS and peripheral immune response in the BTBR mouse model of autism. Neuroscience. 2020;435:22–32.
34. Silverman JL, Tolu SS, Barkan CL, Crawley JN. Repetitive self-grooming behavior in the BTBR mouse model of autism is blocked by the mGluR5 antagonist MPEP. Neuropsychopharmacology. 2010;35:976–89.
35. McFarlane HG, Kusek GK, Yang M, Phoenix JL, Bolivar VJ, Crawley JN. Autism-like behavioral phenotypes in BTBR T+tf/J mice. Genes Brain Behav. 2008;7:152–63.
36. Liao W, Lin JX, Leonard WJ. Interleukin-2 at the crossroads of effector responses, tolerance, and immunotherapy. Immunity. 2013;38:13–25.
37. Wang J, Zhao X, Wan YY. Intricacies of TGF-β signaling in Treg and Th17 cell biology. Cell Mol Immunol. 2023;20:1002–22.
38. Álvarez-Rodríguez L, Martínez-Taboada V, Calvo-Alén J, Beares I, Villa I, López-Hoyos M. Altered Th17/Treg ratio in peripheral blood of systemic lupus erythematosus but not primary antiphospholipid syndrome. Front Immunol. 2019;10:391.
39. Arumugasaamy N, Ettehadieh LE, Kuo CY, Paquin-Proulx D, Kitchen SM, Santoro M, et al. Biomimetic placenta-fetus model demonstrating maternal-fetal transmission and fetal neural toxicity of zika virus. Ann Biomed Eng. 2018;46:1963–74.
40. Bettelli E, Carrier Y, Gao W, Korn T, Strom TB, Oukka M, et al. Reciprocal developmental pathways for the generation of pathogenic effector TH17 and regulatory T cells. Nature. 2006;441:235–8.
41. Jia X, Song Y, Li Z, Yang N, Liu T, Han D, et al. Melatonin regulates the circadian rhythm to ameliorate postoperative sleep disorder and neurobehavioral abnormalities in aged mice. CNS Neurosci Ther. 2024;30:e14436.
42. Zheng Y, Ren Z, Liu Y, Yan J, Chen C, He Y, et al. T cell interactions with microglia in immune-inflammatory processes of ischemic stroke. Neural Regen Res. 2025;20:1277–92.
43. Sakai Y, Shaw CA, Dawson BC, Dugas DV, Al-Mohtaseb Z, Hill DE, et al. Protein interactome reveals converging molecular pathways among autism disorders. Sci Transl Med. 2011;3:86ra49.
44. Thomas SD, Jha NK, Ojha S, Sadek B. mTOR signaling disruption and its association with the development of Autism Spectrum Disorder. Molecules. 2023;28:1889.
45. Arenella M, Mota NR, Teunissen MWA, Brunner HG, Bralten J. Autism spectrum disorder and brain volume link through a set of mTOR-related genes. J Child Psychol Psychiatry. 2023;64:1007–14.
46. Bartolomaeus H, Balogh A, Yakoub M, Homann S, Markó L, Höges S, et al. Short-chain fatty acid propionate protects from hypertensive cardiovascular damage. Circulation. 2019;139:1407–21.

AUTHOR CONTRIBUTIONS

ML, ZN, BL, XC conceptualized and designed the research study. ML, SY, HC, PY, XX, CS conducted the experiments. Statistical analyses were performed by ML and XK. XK and ML wrote the manuscript with major edits from XC. ZL, HZ, JW, XH, JY (Jingrui Yang), JY (Jinyuan Yan), PW provided significant research support. BL and XC supervised the study and obtained funding. All authors reviewed and approved the final manuscript. All authors reviewed and approved the final manuscript.

FUNDING

This research was supported by the National Natural Science Foundation of China (grant no. 82460281, grant no. 82060306), Yunnan Province Biomedical Special Project (grant no. 202402AA310051), the Yunnan Province Li Bin Expert Workstation (grant no. 202305AF150068), and the Yunnan Province Biomedical Major Special Project (grant no. 202102AA100007-4).

COMPETING INTERESTS

The authors declare no competing interests.

ETHICS APPROVAL AND INFORMED CONSENT

All experiments involving animal studies were in accordance with the ethical standards of Laboratory Animal—Guideline for Ethical Review of Animal Welfare. The study was approved by the Ethical Committee for Animal Studies of Kunming Medical University (Approval number: kmmu20220368). This study doesn't involve human studies.

ADDITIONAL INFORMATION

Correspondence and requests for materials should be addressed to Bin Li or Xia Cao.